NEW VISTA OF SHELL STRUCTURE IN NEUTRON-RICH EXOTIC NUCLEI*

H. Grawe

Gesellschaft für Schwerionenforschung
Planckstr. 1, 64291 Darmstadt, Germany

(Received October 29, 2002)

The origin of new shell structure observed in neutron-rich light nuclei and implications for medium-heavy nuclei are discussed in terms of the monopole part of the in-medium NN interaction. The evolution of the harmonic oscillator (HO) closed shells $N = 8, 20, 40$ via shell gap quenching towards $N_m - 2N$, with N numbering HO quanta, is compared to recent experimental data. The locality of the monopole driven shell change and the fading of its shell quenching power beyond $N = 50$ is discussed.

PACS numbers: 21.60.Cs, 21.10.Dr, 27.20.+n, 27.30.+t

1. Introduction

The change of shell structure in neutron-rich nuclei has been subject of numerous theoretical studies [1–4]. With the advent of modern in-flight and ISOL based spectrometers experiments, employing fragmentation and fission of relativistic heavy-ion beams and spallation reactions, provided evidence for shell quenching and evolution of new shells [5–10]. Based on predictions for extreme N/Z ratios [1] shell quenching and reordering are explained by the softening of the nuclear potential in neutron-excessive nuclei. As a consequence *high*$-l$ orbitals are pushed upward and the spin–orbit (SO) splitting, being proportional to the radial derivative of the potential, is reduced. This leads to a transition from a SO determined shell gap ($N = 50, 82, 126$) to shell gaps of the harmonic oscillator (HO) type ($N = 40, 70, 112$) [11]. The scenario is characterised by the sequential *shell quenching* and *reordering*, a transition *SO to HO* gap, *smooth* evolution with N/Z and *reduced* SO splitting. None of these signatures applies to the new shell structure observed in light and medium-heavy nuclei. Therefore, an alternative approach will be outlined in the Sec. 2 and compared to experimental evidence in Sec. 3.

* Presented at the XXXVII Zakopane School of Physics "Trends in Nuclear Physics", Zakopane, Poland, September 3–10, 2002.

2. Monopole driven shell structure

The propagation of single particle energies with increasing occupation of a major shell is governed by the monopole part of the residual interaction [12] as defined by

$$V^m_{jj'} = \sum_J (2J+1)\langle jj'|V|jj'\rangle_J \Big/ \sum_J (2J+1)\,.$$

It has been pointed out that the $(\sigma\cdot\sigma)(\tau\cdot\tau)$ part of the in-medium NN interaction provides the schematic explanation for the enhancement of V^m for proton–neutron ($\pi\nu$) pairs of a factor of 2 relative to $T=1$ pairs and another approximate factor of 2 for spin–orbit partners in the long-range limit [13]. A closer inspection of experimental data in the $N=29$ [14] (Fig. 1(a)), $N=51$ [15] isotones, the $Z=29$ [16] (Fig. 1(b)) and $Z=51$ [17] isotopes, and of realistic interactions derived from effective NN potentials by a G-matrix calculation with core polarisation corrections and fitted to experimental data as summarised in Table I [18–21] reveals V^m to be strong in $\pi\nu$ pairs with total spin $S=0$ and preferably identical number of nodes in their radial wave functions. In fact the selected examples yield the approximate factor of 2 between $S=0$ and $S=1$ configurations. Based

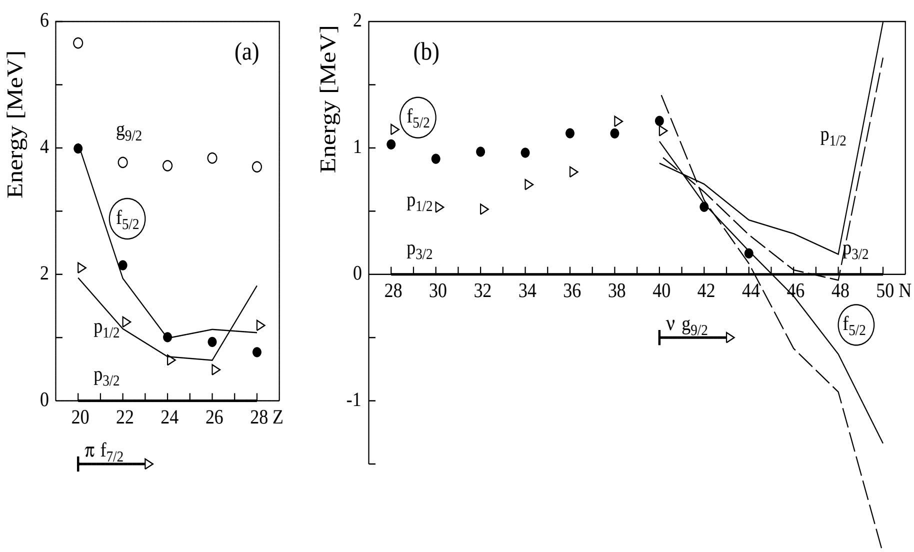

Fig. 1. Monopole migration of neutron single particle states in (a) $N=29$ isotones (^{49}Ca to ^{57}Ni) in comparison to shell model results (full line) with the FPD6 interaction [18] and (b) in $Z=29$ (Cu) isotopes compared to shell model results for the S3V interaction [20] (full line) and scaled to $A=68$ (dashed), respectively.

TABLE I

Monopole strength V^m for multiplets (jj') in $S = 0$ and $S = 1$ configurations and relative monopole shift Δ of orbitals (j_1', j_2') when filling a full j shell.

Multiplet $j, j'_{1,2}$	V^m (MeV)	$\Delta(j'_1, j'_2)$ (MeV)	Interaction Ref.
$\pi f_{7/2} \nu f_{5/2}$	-1.046	4.258	$A = 48$ [18]
$\pi f_{7/2} \nu p_{3/2}$	-0.513		
$\pi f_{7/2} \nu f_{5/2}$	-0.930	3.151	$A = 48$ [19]
$\pi f_{7/2} \nu p_{3/2}$	-0.536		
$\nu g_{9/2} \pi f_{5/2}$	-1.034	5.310	$A = 68$ [20]
$\nu g_{9/2} \pi p_{3/2}$	-0.503		
$\pi g_{9/2} \nu g_{7/2}$	-0.744	4.258	$A = 88$ [21]
$\pi g_{9/2} \nu d_{5/2}$	-0.370		

on this criterion, and considering $S = 0$ pairs to be dominant, the following shell changing scenario emerges when moving from a $N = Z$ doubly magic nucleus as *e.g.* ^{16}O, ^{40}Ca along an isotonic chain to $N \gg Z$ (see insert in Fig. 2):

1. Removing protons from a filled $(n, l, j_< = l - 1/2)$ orbit, as *e.g.* $0p_{1/2}$, $0d_{3/2}$, in a closed shell (CS) will shift the $(n, l + 1, j_> = l + 3/2)$ orbit, as *e.g.* $0d_{5/2}$, $0f_{7/2}$, upward as its binding is weakened relative to the neighbouring orbits, thus swapping positions among them.

2. On removal of further protons from the next lower lying orbit $(n, l, j_> = l+1/2)$, *e.g.* $0p_{3/2}$, $0d_{5/2}$, its spin–orbit neutron partner will be released in a dramatic way to create a new shell CS' (insert Fig. 2).

The effect can be summarised as a change of a HO shell closure with magic number $N_m = 8, 20, 40$ to $N_m - 2 \times N = 6, 16(14), 34(32)$, with N counting the HO quanta. The ambiguity for $N > 1$ is due to the presence of $j = 1/2$ orbits as *e.g.* $s_{1/2}$ or $p_{1/2}$, which strongly mix by pair scattering with the neighbouring higher-spin orbitals (see Secs. 3.1 and 3.2). The scenario is characterised by the following signature, which substantially deviates from the mechanism described in Sec. 1 :

- a HO (ls-closed) shell changes to a SO (jj-closed) shell;
- the change is rapid with subshell occupation, and highly localised;
- the apparent SO splitting is increased.

The according shell structure change is shown in the chart of Fig. 2.

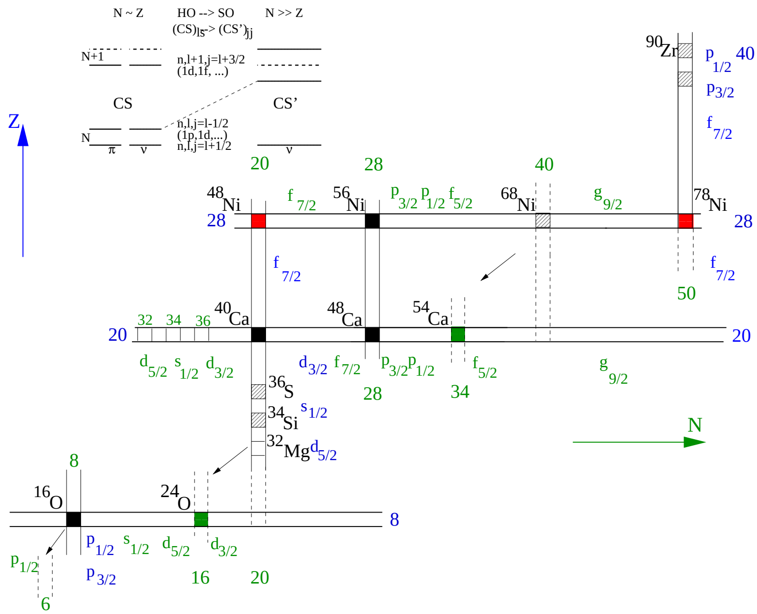

Fig. 2. Schematic chart of known and expected new shell structure in $N \gg Z$ nuclei. The insert illustrates the scenario when moving from $N \sim Z$ to $N \gg Z$.

3. Experimental evidence for new shells

The scenario described in Sec. 2 accounts in a straightforward way for the recently established new shell effects in light and medium-heavy nuclei, which will be reviewed in the following. Besides single particle states, two-nucleon separation energies S_{2n} and S_{2p} and their differences δ_{2n} resp. δ_{2p}, excitation energies E_{2^+} of $I^\pi = 2^+$ states and $B(E2; 2^+ \to 0^+)$ will be used as signatures for shell structure [22].

3.1. The $N = 8$ shell evolution below $Z = 8$

In Fig. 3 the evolution of the $N = 8$ shell gap is illustrated. Removal of the $\pi p_{1/2}$ protons from the doubly magic ^{16}O releases the $\nu d_{5/2}$, $S = 0$ partner neutron and hence the $I^\pi = 5/2^+$ and $1/2^+$ levels swap positions from ^{17}O to ^{15}C (Fig. 3). The neutron shell gap is preserved in ^{14}C as documented by the large E_{2^+} (Fig. 4(a)), which is only marginally smaller than in ^{16}O. This demonstrates the aforementioned ambiguity of shell signature for nuclei separated by a $j = 1/2$ subshell (see also Sec. 3.2). The dramatic decrease of E_{2^+} observed for ^{12}Be (Fig. 4a) indicates that the removal of the first pair of $\pi p_{3/2}$ protons causes an upward shift of the $\nu p_{1/2}$ spin-flip partner level, thus closing the $N = 8$ gap while opening a $N = 6$

gap. This is impressively corroborated by the ^{11}Be level scheme shown in Fig. 3 and the inversion of the I^π=1/2$^+$ and 1/2$^-$ levels. For ^{8}He an estimate for the $N = 6$ shell gap can be inferred from the measured [23] energy difference of the I^π=3/2$^-$; $\nu p^3_{3/2}$ hole and the I^π=1/2$^-$; $\nu p^2_{3/2}p_{1/2}$ particle states. Using the two-body matrix elements (TBME) from Ref. [24] a shell gap $\epsilon(p_{1/2}) - \epsilon(p_{3/2})$= 4.25 MeV is calculated. We mention in passing that the $N = 6$ shell stabilisation makes ^{9}Li a good core for ^{11}Li halo calculations.

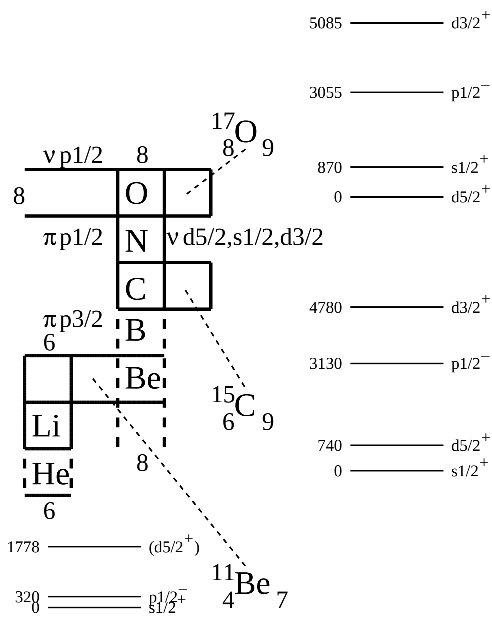

Fig. 3. Shell change $N = 8$ to 6.

3.2. The evolution of the $N = 20, 28$ shells below $Z = 20$

As described in part (1) of the scenario and corresponding to $N = 8$ the removal of $\pi d_{3/2}$ protons from ^{40}Ca stabilises the $N = 20$ shell gap as the $S = 0$ partner orbital $\nu f_{7/2}$ is shifted upward. Consequently, and known since long, ^{36}S and ^{34}Si, again separated by a $j = 1/2(s_{1/2})$ orbit, show doubly magic features (Fig. 4(b)). It would be an experimental challenge to prove the present scenario in the mirror nuclei ^{34,36}Ca, which should exhibit identical shell signature. The upward shift of the $\nu f_{7/2}$ orbital with removal of $\pi d_{3/2}$ protons, on the other hand, quenches the $N = 28$ gap below ^{48}Ca, as exhibited in enhanced $B(E2; 0^+ \to 2^+)$ values measured in Coulomb excitation and the absence of shell closure features in ^{44}S [6].

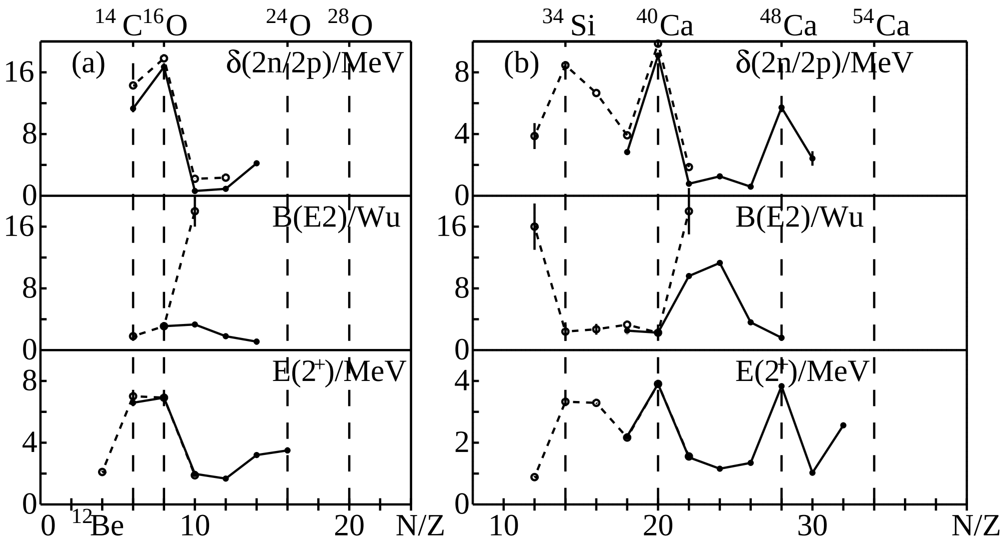

Fig. 4. Shell signatures $\delta_{2n/2p}$, $B(E2; 2^+ \to 0^+)$ and E_{2^+} for shell change between $N = 8$ and 20 along (a) $Z = 8$ (O) isotopes (full line) and $N = 8$ isotones (dashed) and (b) $N = 20$ isotones (dashed) and $Z = 20$ (Ca) isotopes (full line).

Following part (2) of the scenario further removal of $\pi d_{5/2}$ protons in $N = 20$ isotones will shift the $\nu d_{3/2}$ orbital into the shell gap, and, aided by $2p2h$ excitations, drives ^{32}Mg to deformation [5]. The evolution of the $N = 16$ (14) shell below the $\nu d_{3/2}$ orbital is complete in the oxygen isotopes, where ^{22,24}O exhibit large E_{2^+}, small $B(E2)$ and a rise in δ_{2n} (Fig. 4(a)). In a recent shell model study this was reproduced quantitatively, on the expense, however, of an *ad hoc* correction of the realistic interaction employed [13]. The locality of the change in shell structure discussed in the present scenario was proven in a recent experiment showing a decrease in E_{2^+} from ^{22}O (3.20 MeV) to ^{20}C (1.56 MeV) [25]. As stated in Sec. 3.1 this is due to the $\pi p_{1/2}$ removal, which shifts the $\nu d_{5/2}$ level into the $N = 16(14)$ gap.

3.3. The evolution of the $N = 40, 50$ shells

The HO closed shell $N = 40$ in ^{68}Ni is weak and isolated and looses its strength already at two particles/holes distance [22, 26]. Excitation energy E_{2^+} and $B(E2; 0^+ \to 2^+)$ exhibit shell closure [27], while δ_{2n} does not show any effect [22, 26]. Removing $\pi f_{7/2}$ protons from ^{68}Ni prompts the $\nu f_{5/2}$ orbit to move into the (small) $N = 40$ shell gap, so that ^{66}Fe shows features of deformation [28]. This was proven recently by assigning the Nilsson configuration $5/2^+[422]$ to the ground state of ^{67}Fe [29]. Correlated to this upward shift of the $\nu f_{5/2}$ orbit a $N = 34$ gap opens above the

$\nu p_{3/2}, p_{1/2}$ levels as also exhibited by the $N = 29$ single particle states at $Z = 20$ (Fig. 1(a)). The presence of the $p_{1/2}$ orbit introduces the $N = 34(32)$ ambiguity. Experimentally a large E_{2^+} is observed in ^{52}Ca [10] and shell gaps are established in the yrast spectrum of the ^{52,54}Ti isotopes [30].

The persistence of the $N = 50$ shell gap at ^{78}Ni is discussed since long [1, 22]. As the last measured value is known for Se ($Z = 34$), removal of the last $\pi f_{5/2}$ protons in the light of monopole driven shell structure is essential, as the $\pi f_{5/2} \nu g_{9/2}$ monopole is known to be strong [16] which is reproduced by realistic interactions (Fig. 1(b), Table I). Starting from ^{84}Se for $N = 50$ and ^{68}Ni for $Z = 28$ the ^{78}Ni shell gaps can be estimated as summarised in Table II. The gaps are determined by V^m in the configurations $\pi f_{5/2} \nu g_{9/2}$ and $\pi f_{5/2} \nu d_{5/2}$ for $N = 50$ and $\pi f_{5/2} \nu g_{9/2}$ and $\pi f_{7/2} \nu g_{9/2}$ for $Z = 28$, respectively. Assuming the empirical factor of 2 between $S = 0$ and $S = 1$ monopoles (Table I), the relative monopole shift of two orbitals j_1', j_2' as given by

$$\Delta(j_1', j_2') = (V^m_{jj_1'} - V^m_{jj_2'})\ (2j+1)$$

with $(j_1', j_2') = (\nu g_{9/2}, \nu d_{5/2})$ and $(\pi f_{5/2}, \pi f_{7/2})$ and $j = \pi f_{5/2}$ and $\nu g_{9/2}$, respectively, can be estimated. The results listed in Table II for various interactions yield a substantially reduced but still appreciable $N = 50$ gap, while the $Z = 28$ gap is well preserved. It should be noted, that these estimates do not include cross-shell interactions and mutual enhancement of proton and neutron shell and therefore represent lower limits only. Therefore it is expected that the $I^\pi = 8^+$ isomerism observed at the beginning of the $\nu g_{9/2}$ shell in ^{70}Ni [31] and in ^{78}Zn [32] is preserved for ^{76}Ni. In a recent experiment evidence for the latter has been found [33].

TABLE II

$N = 50$ and $Z = 28$ shell gap extrapolation to ^{78}Ni.

$Z-28$ occ. $\pi f_{5/2}$	$N = 50$ shell gap (MeV)	$N-40$ occ. $\nu g_{9/2}$	$Z = 28$ shell gap (MeV)	Ref.
6	4.13(4)	0	5.91(26)	^{84}Se/^{68}Ni
0	2.08	10	4.46	$A = 68$ [20]
	2.60		4.39	$A = 100$ [20]
	2.56		3.58	exp. fit

4. Conclusions

It has been demonstrated that monopole migration can account qualitatively for new shell structure and its signatures in neutron-rich nuclei up to $N = 50$, while beyond its strength due to the $A^{-1/3}$ scaling has little impact on shell structure. It is worth noting that neither large scale shell model nor mean field calculations have predicted this change in shell structure. For realistic interactions used in large scale shell model calculations it is known that they account poorly for the monopole strength and need *ad hoc* corrections to reproduce the propagation of single particle energies [12, 13]. Moreover, to account for a change in HO shell structure realistic interactions consistent in two adjacent HO major shells have to be derived. For mean field interactions it has been argued recently that they may fail to account for the $(\sigma \cdot \sigma)(\tau \cdot \tau)$ part of the NN interaction [13].

REFERENCES

[1] J. Dobaczewski *et al.*, *Phys. Rev. Lett.* **72**, 981 (1994).

[2] G.A. Lalazissis *et al.*, *Phys. Lett.* **B418**, 7 (1998).

[3] P.G. Reinhard *et al.*, *Phys. Rev.* **C60**, 014316 (1999).

[4] E. Caurier *et al.*, *Phys. Rev.* **C58**, 2033 (1998).

[5] T. Motobayashi *et al. Phys. Lett.* **B346**, 9 (1995).

[6] T. Glasmacher *et al. Phys. Lett.* **B395**, 163 (1997).

[7] T. Aumann *et al.*, *Phys. Rev. Lett.* **84**, 35 (2000).

[8] V.A. Navin *et al.*, *Phys. Rev. Lett.* **85**, 266 (2000).

[9] P.G. Thirolf *et al.*, *Phys. Lett.* **B485**, 16 (2000).

[10] A. Huck *et al.*, *Phys. Rev.* **C31**, 2226 (1985).

[11] B. Pfeiffer *et al.*, *Nucl. Phys.* **A693**, 282 (2001).

[12] E. Caurier *et al.*, *Phys. Rev.* **C60**, 225 (1994).

[13] T. Otsuka *et al.*, *Eur. Phys. J.* **A13**, 69 (2002) and *Phys. Rev. Lett.* **87**, 082502 (2001).

[14] Evaluated Nuclear Structure Data File `http://www.nndc.bnl.gov/nndc/ensdf/`

[15] H. Grawe *et al.*, *Nucl. Phys.* **A704**, 211c (2002).

[16] S. Franchoo *et al.*, *Phys. Rev.* **C64**, 054308 (2001).

[17] A. Covello, private communication.

[18] W.A. Richter *et al.*, *Nucl. Phys.* **A523**, 325 (1991).

[19] T.T.S. Kuo, G.E. Brown, *Nucl. Phys.* **A114**, 241 (1968).

[20] J. Sinatkas *et al.*, *J. Phys. G* **18**, 1377 and 1401 (1992).

[21] M. Hjorth-Jensen *et al.*, *Phys. Rep.* **261**, 125 (1995).

[22] H. Grawe, M. Lewitowicz, *Nucl. Phys.* **A693**, 116 (2001).

[23] H. Emling, *Acta Phys. Pol. B* **34**, 2323 (2003), these Proceedings.

[24] S. Cohen, D. Kurath, *Nucl. Phys.* **A101**, 1 (1967).

[25] F. Azaiez, Proc. NS2002, Berkeley, to be published in AIP Conf. Proc.; M. Lewitowicz, not submitted to the Proceedings.

[26] H. Grawe *et al.*, *Proc. Tours 2000, AIP* **CP561**, 287 (2001).

[27] O. Sorlin *et al.*, *Phys. Rev. Lett.* **88**, 092501 (2002).

[28] M. Hanawald *et al.*, *Phys. Rev. Lett.* **82**, 1391 (1999).

[29] M. Sawicka *et al.*, *Eur. Phys. J.* **A**, in print.

[30] R.V.F. Janssens *et al.*, *Phys. Lett.* **B546**, 55 (2002).

[31] R. Grzywacz *et al.*, *Phys. Rev. Lett.* **81**, 766 (1998).

[32] J.M. Daugas *et al.*, *Phys. Lett.* **B476**, 213 (2000).

[33] M. Sawicka *et al.*, Proc. NS2002, Nuclear structure with large gamma-arrays, Padova, Sept. 23-27, 2002, to be published in *Eur. Phys. J.* **A**.